THEORETICA CHIMICA ACTA
Theoret. Chim. Acta (Berl.) 63, 269–290 (1983)


*Original Investigations*

# Location of Transition States and Stable Intermediates by MINIMAX/MINIMI Optimization of Synchronous Transit Pathways

Axel Jensen

Institut für Organische Chemie der Johannes Gutenberg-Universität,
Johann-Joachim Becher Weg 18–20, D-6500 Mainz, Federal Republic of Germany

The MINIMAX/MINIMI concept for the location of transition states and/or stable intermediates of chemical reactions is introduced, based on the synchronous transit method. According to this strategy, minimization of quadratic synchronous transit path maxima or minima is achieved by constrained exhaustive optimization of internal coordinates. The method and its efficiency are demonstrated for two-dimensional model surfaces as well as for thermally allowed electrocyclic interconversions of cyclopropyl-/allyl-cation and cyclobutene-/butadiene (gauche) within the framework of MNDO-SCF calculations. Thus, in both cases a direct comparison with the exact solution determined by minimization of the scalar gradient norm and cross reference to the original work of Halgren and Lipscomb [3] is possible.

**Key words:** MINIMAX/MINIMI optimization – Location of transition states – Stable intermediates.

## 1. Introduction

Powerful (mini-)computers and many sophisticated and well-tested programs [1,2] are becoming more and more available. It will become increasingly attractive for organic chemists to study and solve problems of chemical reaction mechanisms or chemical reactivity. For this reason attention is drawn to those problems which concern the direct calculation of chemical reactions:

- Determination of minimum energy conformations of all reacting species.
- Location of transition states.

- Identification of intermediates.
- Approximation of the minimum energy path (intrinsic reaction coordinate).

At present, only the first problem can be handled routinely with programs currently in common use [1,2], and the other problems must be regarded as research topics.

Two-dimensional model surfaces can lead to uneconomic or even misleading performance in all currently used methods [4, 5]. It will be shown here that introduction of the new MINIMAX/MINIMI search strategy within the context of synchronous transit approach leads to further improvement of this method in such a way that transition states and/or stable intermediates can be located with more certainty. As a by-product of this modification, more information about the shape of the energy-hypersurface under investigation is available and this may be successfully used to break up the total reaction path into smaller pieces by means of path segmentation.

MINIMAX/MINIMI optimization is subsequently used to locate transition states and local intermediates on two-dimensional model surfaces. Agreement of the results with those of an exact minimization of the gradient norm for the same SCF method (MNDO [6]) is found for the well-known electrocyclic reactions of cyclopropyl-cation and of cyclobutene.

## 2. The Synchronous Transit Method

Halgren and Lipscomb [3] developed the concept of sychronous transit to locate reaction paths and transition states almost simultaneously and without the need to calculate energy gradients. For some unimolecular reaction the underlying principles are explained as far as necessary:

According to the principle of least motion (PLM, [7]) optimized structures of reactant and product are reorientated relative to each other by means of rigid transitions and rotations in such a way that the sums of squares of all coordinate differences for corresponding atoms reaches a minimum. This PLM orientation is displayed in Fig. 11 for the thermally allowed ring opening of cyclobutene (discussed later in detail). Since reaction in both directions will require simultaneous variation of all intramolecular atomic distances between their path-limiting structures, a reasonable definition for the path coordinate PC must be found as a measure of "reaction route" in accordance with this condition. On defining the rms differences DR (for reactant) and DP (for product) in cartesian coordinates at maximum coincidence [7] for each intermediate structure, a simple measure for the distance to the path-limiting structures is obtained.

$$\begin{aligned} \mathrm{DR} &= \left[ 1/N \sum_{j=1}^{N} (x_j^{\mathrm{PLM}} - x_j^R)^2 + (y_j^{\mathrm{PLM}} - y_j^R)^2 + (z_j^{\mathrm{PLM}} - z_j^R)^2 \right]^{1/2} \\ \mathrm{DP} &= \left[ 1/N \sum_{j=1}^{N} (x_j^{\mathrm{PLM}} - x_j^P)^2 + (y_j^{\mathrm{PLM}} - y_j^P) + (z_j^{\mathrm{PLM}} - z_j^P)^2 \right]^{1/2} \end{aligned} \tag{1}$$

where $N$ = number of atoms, $x_j^P$, $y_j^P$, $z_j^P$ = cartesian PLM-coordinates of the product molecules. Using these quantities the path coordinate PC can now be taken as

$$\mathrm{PC} = \mathrm{DR}/(\mathrm{DR}+\mathrm{DP}) \tag{2}$$

for any intermediate structure.

As mentioned above, all intramolecular distances $R_{jk}$ must vary simultaneously between those for path-limiting structures $R_{jk}^R$ and $R_{jk}^P$. For this reason provision can be made to meet one of the following two conditions without limitation of the method:

(a) linear variation:

$$R_{jk}^{(i)} = R_{jk}^R + f(R_{jk}^P - R_{jk}^R) \qquad 0 \le f \le 1; \quad j < k = 1, N \tag{3}$$

(b) parabolic variation [8]:

$$R_{jk}^{(i)} = a + b \cdot f + c \cdot f^2 \qquad 0 \le f \le 1; \quad j < k = 1, N \tag{4}$$

$$a = R_{jk}^R$$

$$b = R_{jk}^P - R_{jk}^R - c$$

$$c = [R_{jk}^M - (1-\mathrm{PM})R_{jk}^R - \mathrm{PM} \cdot R_{jk}^P]/(\mathrm{PM}(\mathrm{PM}-1))]$$

These values ensure that the following conditions are fulfilled:

$$f = 0 \qquad R_{jk}^{(i)} = R_{jk}^R$$

$$f = 1 \qquad R_{jk}^{(i)} = R_{jk}^P$$

$$f = \mathrm{PM} \qquad R_{jk}^{(i)} = R_{jk}^M$$

where PM denotes the value for the path coordinate, $\{R_{jk}^M \mid j < k = 1, N\}$ are the associated atomic distances of some intermediate structure on the path and $(i)$ refers to interpolated quantities.

Using Eq. (3) or Eq. (4) idealized geometries of the so-called synchronous transit path may be calculated easily in terms of interatomic distances $\{R_{jk}^{(i)} \mid j < k = 1, N\}$, which may be used to calculate cartesian coordinates for SCF calculations by means of a "least squares fit". In practice linearly/parabolically interpolated cartesian coordinates $C$ between path-limiting structures at maximum coincidence are subsequently refined so as to minimize the function

$$\sum_{j=1}^{N-1} \sum_{k=j+1}^{N} [R_{jk}^{(i)} - R_{jk}^{(c)}]^2/[R_{jk}^{(i)}]^4 + 10^{-6} \times \sum_{w=x,y,z} \sum_{j=1}^{N} [w_j^{(i)} - w_j^{(c)}]^2 \tag{5}$$

where $(i)$ = interpolated, $(c)$ = calculated. The calculated quantities $(c)$ refer to the (updated) calculated cartesian coordinates $C$ and all quantities are measured in atomic units. The weighting factor $[1/R_{jk}^{(i)}]^4$ for the squares of distance differences ensures a close reproduction of bond distances whereas the weighting

factor $10^{-6}$ is proposed to suppress rigid translations and rotations for a determinate fit. This procedure can be used for molecules with $N > 3$ since the number of $\binom{N}{2}$ interatomic distances exceed the number of $3N-6$ internal degrees of freedom for a nonlinear molecule.

Each transit structure $C$ is then submitted to PLM to associate a unique path coordinate according to (2). Then $C$ is transferred to the SCF program in use, in order to calculate the corresponding total energy. Variation of $f$ $(0 \leq f \leq 1)$ thus produces a continuous energy path $E(\mathrm{PC})$ which is called linear synchronous (LST, (3)) or quadratic synchronous transit path (QST, (4)). In the case of a unimolecular reaction, this path will usually connect both limiting structures via some path maximum at PC = PCMAX, whose structure can be determined using Eqs. (4) and (5) in the manner described. Exhaustive application of some constrained minimization procedure (to avoid the collapse to local minima of reactant/product) will allow the approach to the relevant saddle point. If this condition is met, a first approximation of the reaction path is gained simultaneously via Eq. (4) and can subsequently be refined by application of similar optimization techniques to selected geometries along this path to yield a multi-segment-path.

## 3. The Constraint of Constant Path Coordinate (Orthogonal Optimization)

This constraint [3b] is based on reducing the complex search for saddle points to two independent one dimensional search procedures in a special curvilinear coordinate system which is especially well suited for chemical purposes. For the case of two dimensions this means:

1. Eq. (4) defines a parabolic network of transit paths with the special case of (3) for $c = 0$ (the LST path). Along these paths, maxima of total energy are determined by means of parabolic interpolation.

2. The constraint $\mathrm{PC} = \mathrm{DR}/(\mathrm{DR}+\mathrm{DP}) = \text{const.}$ represents a network of non-concentric circles which are grouped symmetrically about reactant and product [9]. Along these curves, minima of total energy are calculated by parabolic interpolation.

The saddle point is reached if the crossing point of both curve-types simultaneously corresponds to a true maximum for 1 and a minimum for 2.

This strategy proves to be successful in the case of a two-dimensional model surface (Fig. 1), as well as for the thermally allowed electrocyclic ring opening of the cyclopropyl-cation [3b]. Nevertheless, successful exploration of the more complex hypersurface for the homologous reaction of cyclobutene fails if no additional features [10] are incorporated into the search strategy. One of these, called path segmentation, is given [3b] without further justification. As will be demonstrated for a more complex two-dimensional model, path segmentation is an essential feature of the method to guarantee convergence to the saddle point. In special cases, however, it can be ignored, if the concept of orthogonal optimization is replaced by the new MINIMAX technique (refer to Chap. 6.2).

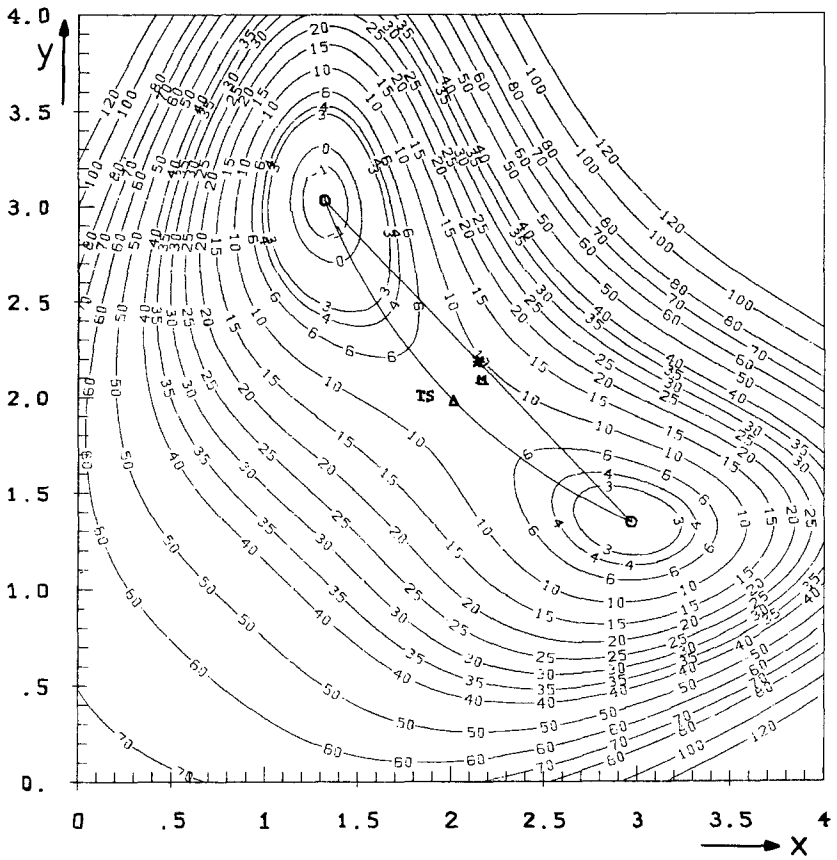


**Fig. 1.** Contour diagram of the model function. $E = ((x-y)^2-(5/3)^2)^2+4(xy-4)^2+x-y$. $M$ = LST1-maximum (start of MINIMAX-optimization). TS = Transition state

## 4. The MINIMAX-/MINIMI-Procedure for Location of Transition States and Stable Intermediates

The concept of orthogonal optimization for the location of saddle points suffers from one severe disadvantage: in the course of an orthogonal optimization of a path maximum the original destination to locate an energetically improved QST maximum is not taken explicitly into account. Unfortunately, renewed exhaustive orthogonal optimization of the resulting QST maximum is not sufficient to force convergence to the saddle point. This has been proved elegantly [5] for the model surface (Figs 3 and 5) and has basically geometric reasons: a simple parabolic transit path cannot provide a correct description of the true minimum energy path if this path shows frequently changing sign of curvature. By means of path segmentation these difficulties can be avoided if proper conditions for the selection of path-limiting structures (which replace corresponding terms in Eq. (3) or (4)) can be developed.

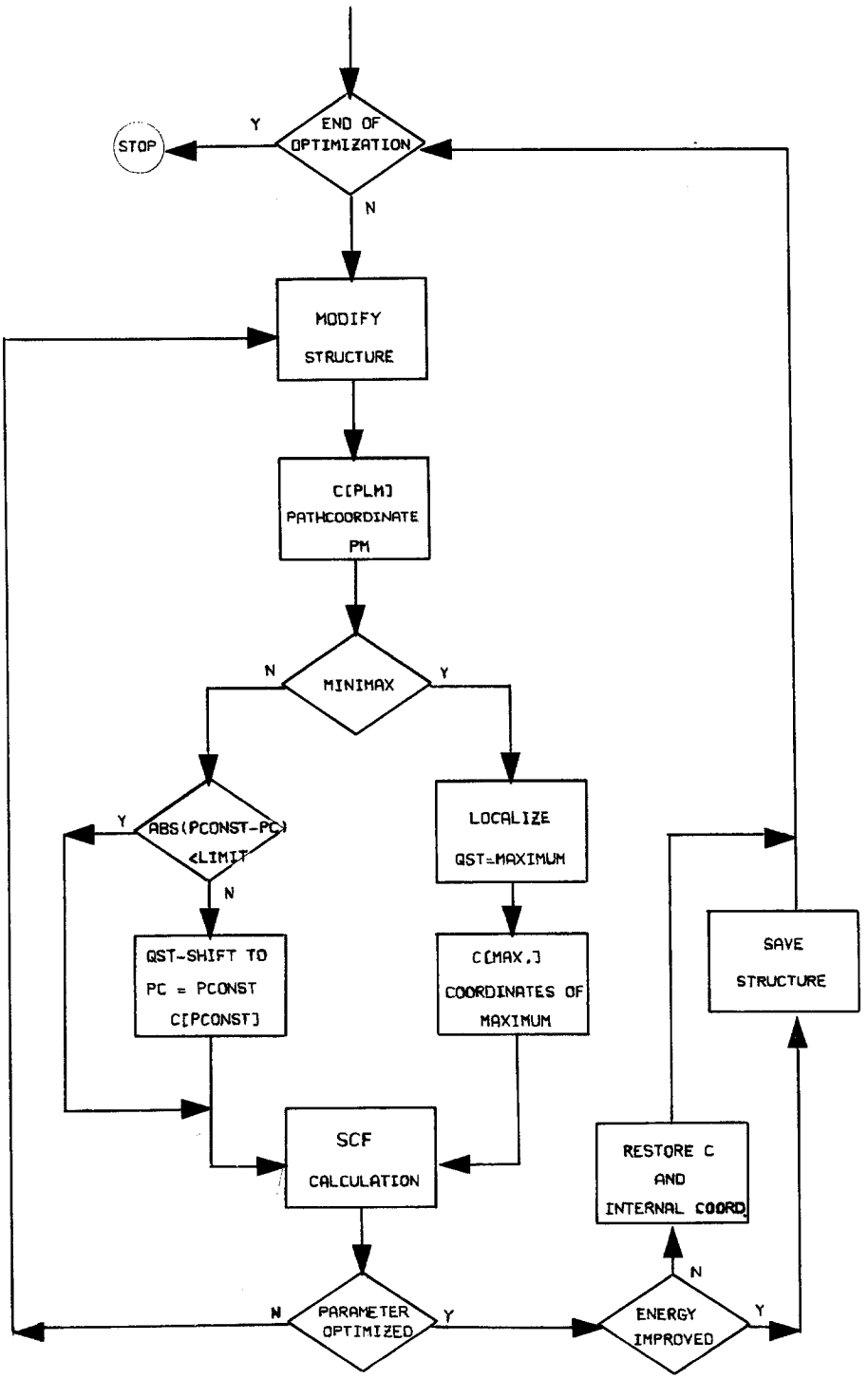


**Scheme 1.** Flow diagram for the orthogonal and MINIMAX optimization

One essential supposition requests to drop the constraint of constant path coordinate in the context of saddle point location: it must be considered as uneconomic to find a new QST maximum with higher energy after exhaustive orthogonal minimization. As a consequence, any method which is claimed to avoid these drawbacks, must explicitly take into account the influence of each geometric modification on the new transit path maximum. From several possible ways to do this, the most straightforward concept will be explained: any change in that structure corresponding to the transit maximum (minimum) under investigation will be accepted only if the resulting new path maximum (minimum) is of lower energy. Successive optimization of all internal coordinates within a given symmetry constraint will consequently lead to the lowest QST maximum (the transition state) or minimum (=intermediate) and is therefore called MINIMAX (MINIMI) optimization. Thus, at any time the best approximation is available to the transition state (or intermediate), to its path coordinate and

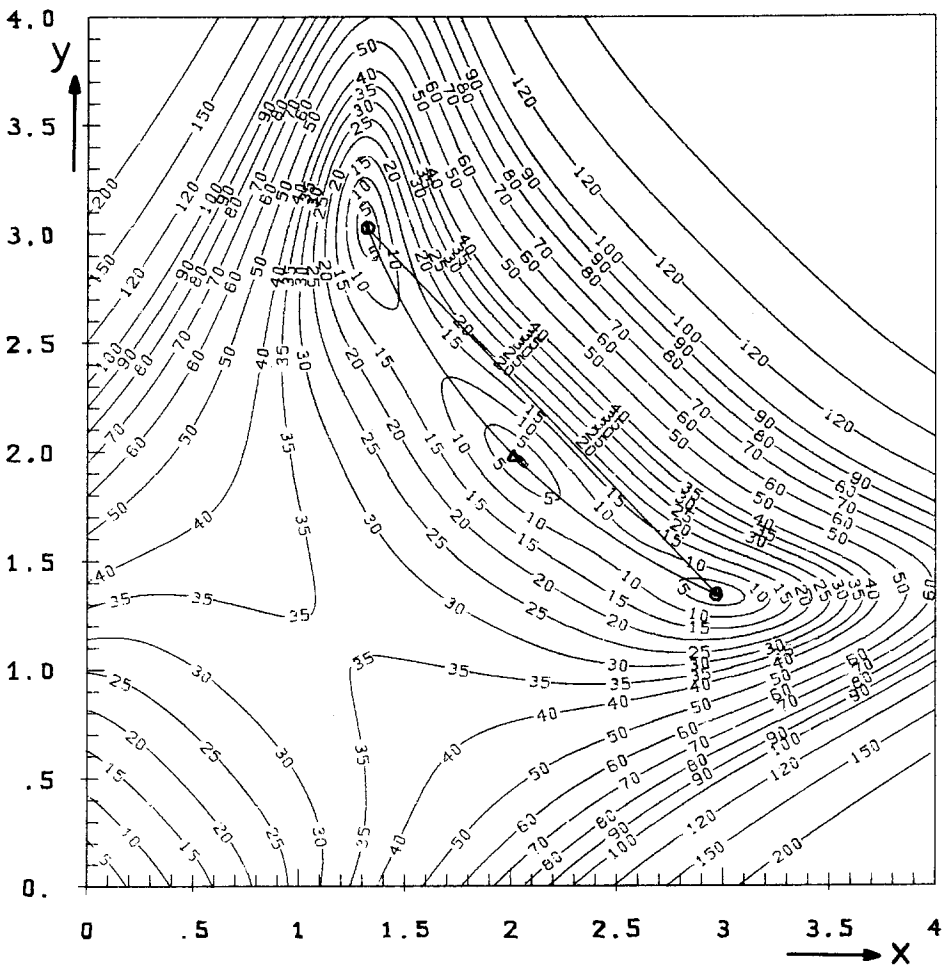


**Fig. 2.** Contour diagram of the gradient norm for the function given in Fig. 1

to the curvature of the corresponding QST path in the vicinity of this point. Unfortunately this demands an additional parabolic line minimization along the QST path at each level of the parameter optimization; however, as a by-product of this procedure, hints to possible or unexpected intermediates (in the case of MINIMAX) or to extreme shifts of the path coordinate may be obtained and these should be regarded as a serious demand for path segmentation and modification of step size for parameter optimization. In Scheme 1 it is shown by means of a flow diagram that orthogonal and MINIMAX optimization can be easily incorporated into one common program unit.

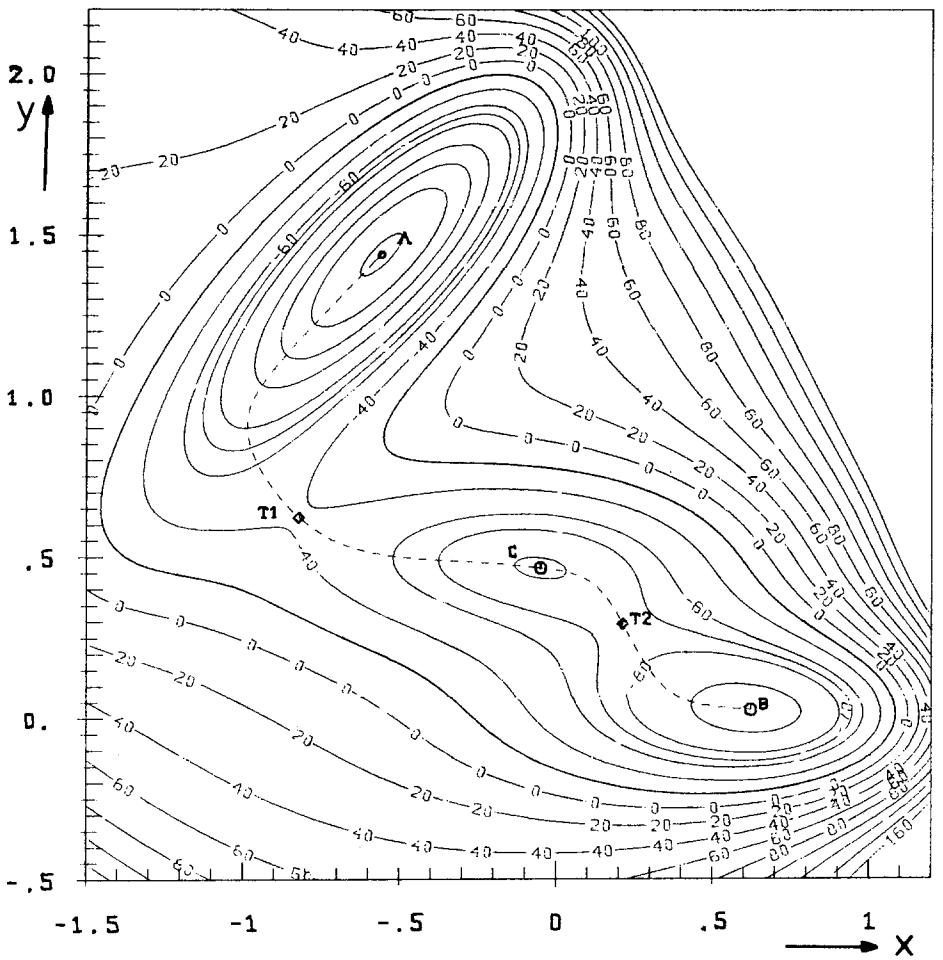


**Fig. 3.** Contour diagram of

$$E = \sum_{i=1}^{4} A_i \exp\left(a_i(x - x_i^0)^2 + b_i(y - y_i^0)(x - x_i^0) + c_i(y - y_i^0)^2\right)$$

$A_i = (-200, -100, -170, 15)$ $\quad c_i = (-10, -10, -6.5, 0.7)$

$a_i = (-1, -1, -6.5, 0.7)$ $\quad x_i^0 = (1, 0, -0.5, -1)$

$b_i = (0, 0, 11, 0.6)$ $\quad y_i^0 = (0, 0.5, 1.5, 1)$

## 5. Tests on Two-Dimensional Model Surfaces

The original model of Halgren and Lipscomb [3b] is given in Fig. 1. Starting with the LST maximum $M$ (marked by $\times$) the result of the MINIMAX optimization (transition state, triangle) and the corresponding QST path is shown. By means of the contour diagram (Fig. 2) for the corresponding gradient norm, correct performance can be demonstrated without further calculation. Obviously this model represents no severe test for either method, orthogonal or MINIMAX optimization.

A greater challenge for the methods will be given by the model surface displayed in Figs 3 and 4 [4, 5]. This has been constructed in such a way that only flexible (and costly) strategies will be successful in this case. Fig. 5 illustrates its complexity via the corresponding contour diagram of the gradient norm which allows identification of two transition states (squares), three absolute minima (solid circles) and several embarrassing local minima ($\times$) for the gradient norm in the vicinity of the presumed transition state. Figure 6 documents the problem which has been discussed in detail in section 4: The true "steepest-descent" path, which was calculated according to the method of "intrinsic reaction coordinate"of Ishida et al. [12], is shown with dashed lines. Starting with minimum $A$ it passes via the saddle point $T1$ to a local intermediate $C$ (true minimum), from there

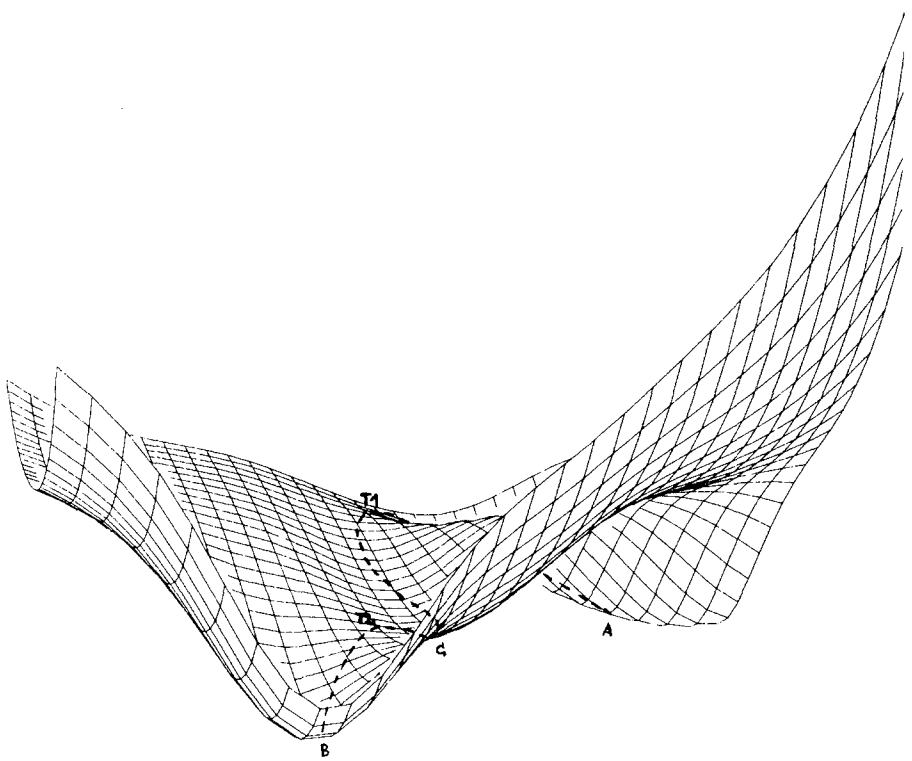


**Fig. 4.** Three-dimensional plot of the function given in Fig. 3

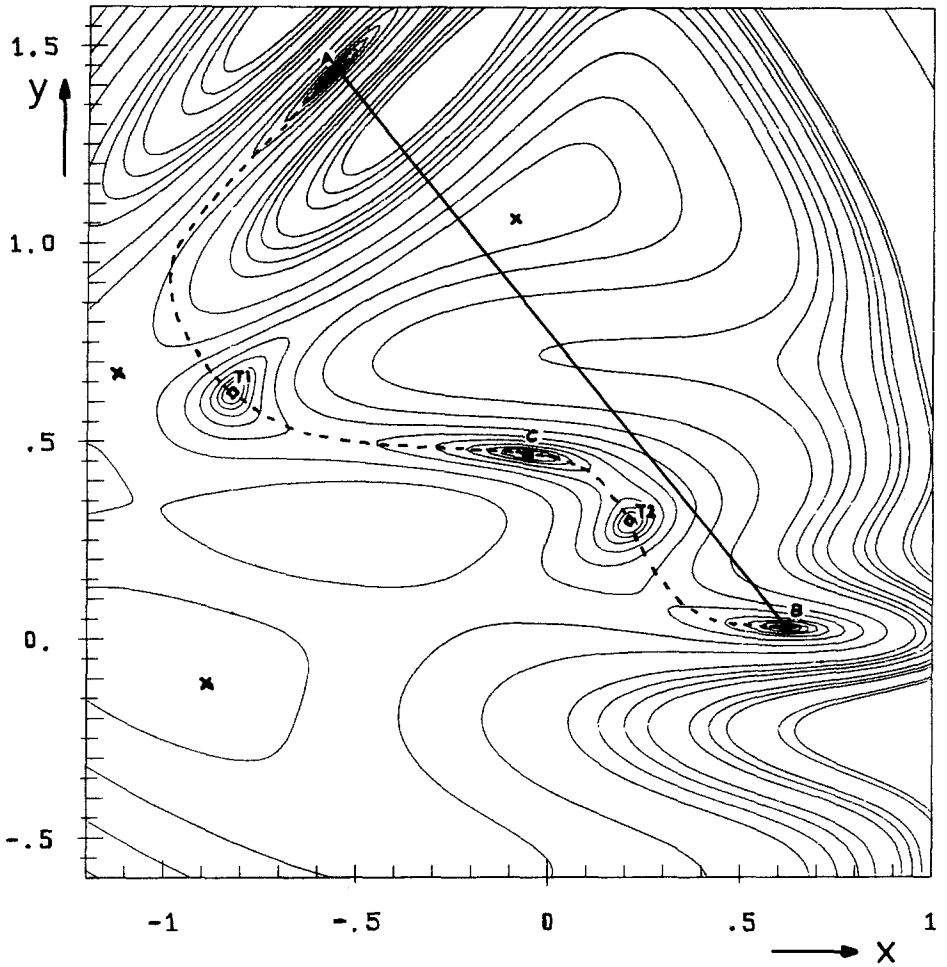


**Fig. 5.** Contour diagram for the gradient norm of the function given in Fig. 3. ● = Null minima, × = local minima, □ = saddle points

to a second transition state $T2$ and finally reaches the "product" minimum $B$. One can immediately see that this path cannot be described with a single parabolic transit path. As a consequence, in an optimization run within the unsegmented path, only one saddle point (or intermediate) can be determined, regardless of the fact that only a poor description of the path is possible (Fig. 6, Table 1). If, however, a correct performance of the synchronous transit concept is guaranteed, transition states, intermediate and the true pathway can be located as close as desired.

From this point of view, exploration of this model should be done as follows:

Starting with the LST1 path connecting minima $A$ and $B$ (straight line $AB$ in Figs. 6 and 8) yields curve 1 (Fig. 7). Careful inspection of this path reveals two maxima separated by a shallow minimum, and the correspondent path coordinates and geometries are determined by parabolic interpolation. The existence

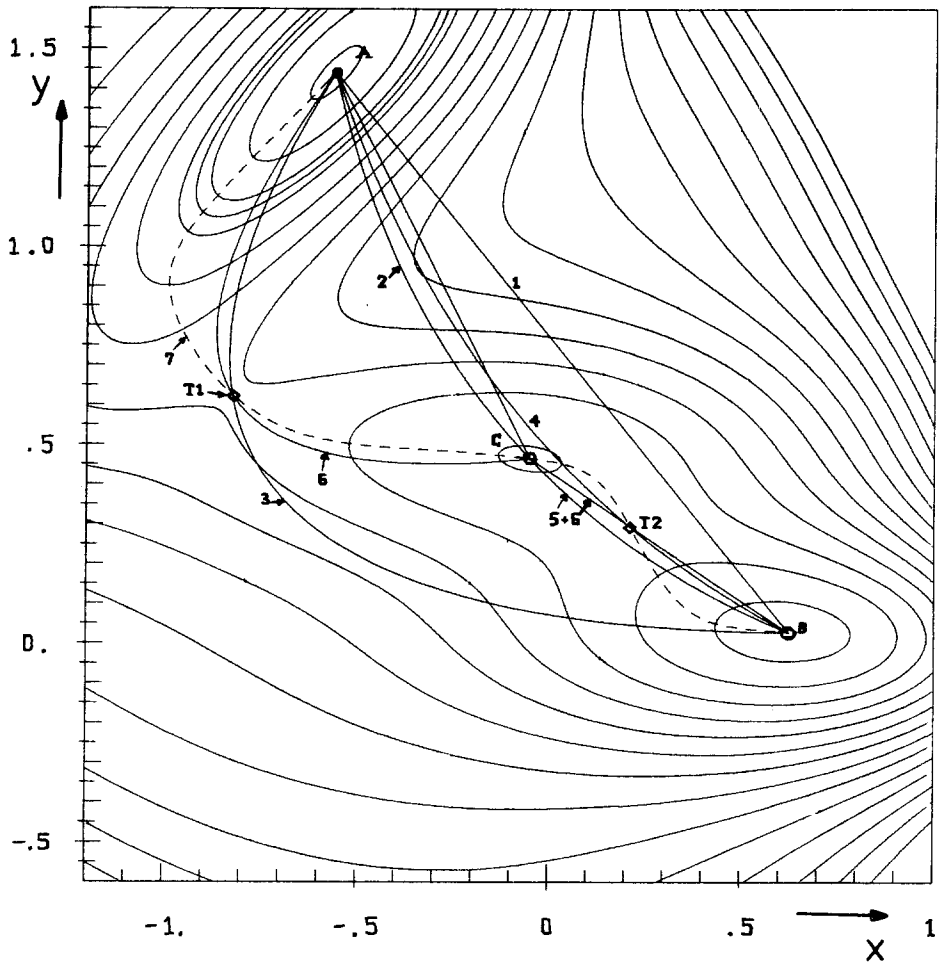


**Fig. 6.** LST and QST paths on the model surface between the local minima *A*, *C* and *B*. *T*1, *T*2 = Transition states. Numbers refer to the transit paths (energy curves) of Fig. 7

of a local minimum in the LST1 path must be regarded as a strong hint for a local intermediate (the minimum *C*) and hence for path segmentation. A hasty orthogonal optimization of one of the two maxima without further test for a minimum would be in error; indeed, total failure would result in this case [5]. Maximal efficiency, however, will be achieved if further refinement of the local minimum structure is attempted by means of a MINIMI optimization [13]. In this case the (unknown) minimum *C* is found (Table 1), and the resulting QST path (Fig. 7, 2nd curve) shows significantly improved maxima which could be used profitably as starting points for optimization runs in a segmented path. Clearly, at this level of calculation path segmentation is indispensable and the overall path *A*–*B* is replaced by two separate segments *A*–*C* and *C*–*B*. The corresponding segment LST paths are shown in Figs 6 and 8 as straight lines and in Fig. 7 as curve 5. Each of these segments has only one maximum, which is located precisely to start the MINIMAX optimizations.

Results of the prescribed optimization runs are given in Table 1 together with those published in Ref. [4].

**Table 1**

| Segment | Opt. point | Result | | | | Ref. [4] | | | |
|---|---|---|---|---|---|---|---|---|---|
| | | $x$ | $y$ | $E$ | $n$ | $x$ | $y$ | $E$ | $n$ |
| $A$–$B$ | $T1$ | —[a] | —[a] | —[a] | —[a] | −0.82 | 0.62 | −40.67 | 124 |
| $A$–$B$ | $T2$ | 0.210 | 0.297 | −72.26 | 218[b] | — | — | — | — |
| $A$–$C$ | $C$ | 0.049 | 0.466 | −80.77 | 64 | — | — | — | — |
| $A$–$C$ | $T1$ | −0.822 | 0.622 | −40.67 | 80 | −0.82 | 0.62 | −40.67 | 113 |
| $C$–$B$ | $T2$ | 0.213 | 0.293 | −72.25 | <32 | 0.22 | 0.29 | −72.26 | 74 |

[a] See text, $n$ = number of function evaluations
[b] Optimization inefficient because steplength (0.1) has been kept constant despite of the vicinity of minimum $C$

Exact solutions:

| Opt. point | $x$ | $y$ | $E$ |
|---|---|---|---|
| $A$ | −0.588 | 1.442 | −146.700 |
| $B$ | 0.623 | 0.028 | −108.167 |
| $C$ | −0.050 | 0.467 | −80.768 |
| $T1$ | −0.822 | 0.624 | −40.665 |
| $T2$ | 0.212 | 0.293 | −72.249 |

If path segmentation is not applied, MINIMAX fails to locate $T1$ because at this point and its close surrounding no true path maximum can be found within the total path $A$–$B$ (Fig. 7, curve 3).

With the results of Table 1 the reaction path is best described by two QST segment paths $A$–$T1$–$C$ and $C$–$T2$–$B$. Despite of a good approximation of the true energy path (Fig. 7, curve 6) relatively large geometric discrepancies may still occur (Fig. 8). These can be easily reduced by orthogonal optimization of two (or more) path structures lying on opposite sides of the transition state (denoted by $P1$–$P4$ in Fig. 8). The resulting structures 01–04 can be used to define significantly improved multi-segment transit pathways (Fig. 8 and Fig. 7, curve 8) and so on.

## 6. MINIMAX Optimization on MNDO [17] Energy Hypersurfaces

The following two reactions are especially well studied. The reader who is interested in a more complete comparison is referred to [6] and references therein.

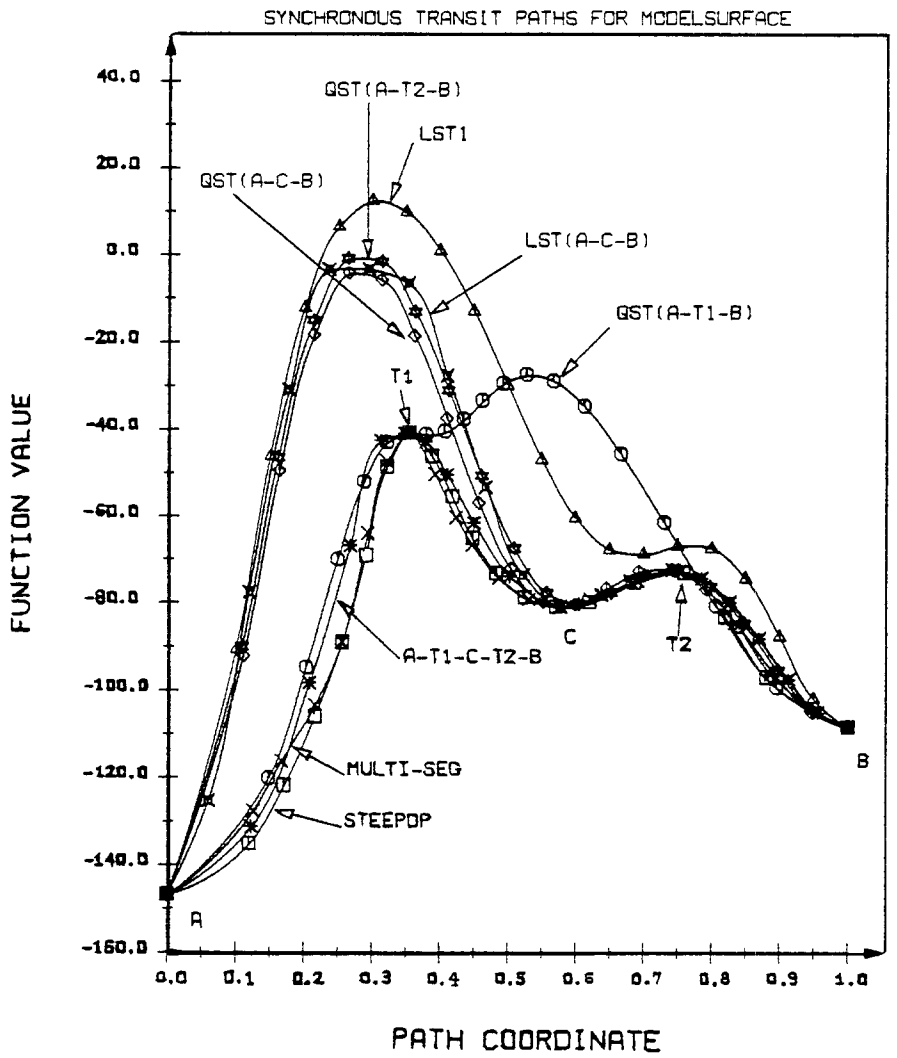


**Fig. 7.** Synchronous transit paths for the corresponding geometry pathways on the model surface given in Figs. 6 and 8

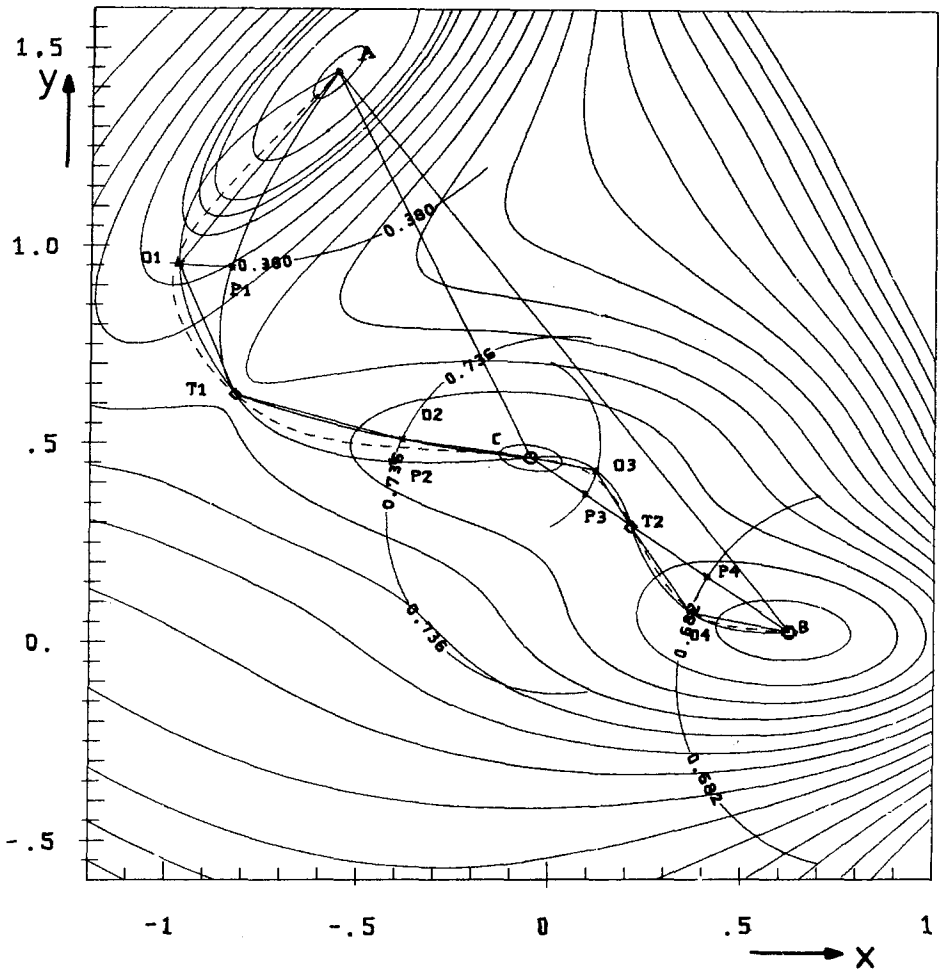


**Fig. 8.** Approximation of the steepest-descent path (dashed lines). Orthogonal optimization of selected points ($P1$–$P4$) of the QST paths through the transition states is used to construct improved multi-segment-paths through the optimized points 01–04

### *6.1. Cyclopropyl-Cation → Allyl-Cation [15]*

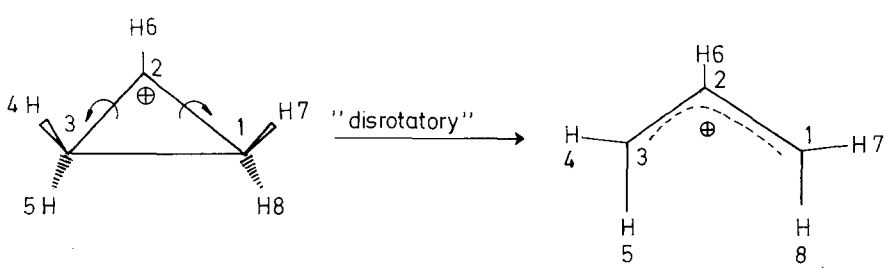


Results for the calculated activation energies and for skeleton data of the transition state are given in Tables 2 and 3.

**Table 2**

| Activation energy (kcal/mole) | SCF procedure | Strategy |
|---|---|---|
| 4.9[a] | MNDO [16] | MINIMAX [16] |
| 4.6[a] | MNDO [6] | Gradient norm |
| 7.6[a] | PRDDO [3b] | Orthog. opt. |

[a] For ring opening, calculated as the difference of total energies (heats of formation) for transition state and reactant

**Table 3**

| Variable | MINIMAX | Ref. [6] |
|---|---|---|
| C1C2 | 1.430 | 1.430 |
| C1C3 | 1.742 | 1.757 |
| H7C1C2 | 119.1 | 119.0 |
| H8C1C2 | 126.1 | 126.5 |

C*i*C*j* = atomic distance C*i*–C*j* in Angström
H*i*C*j*C*k* = angle between atoms H*l*, C*j*, C*k* in degrees

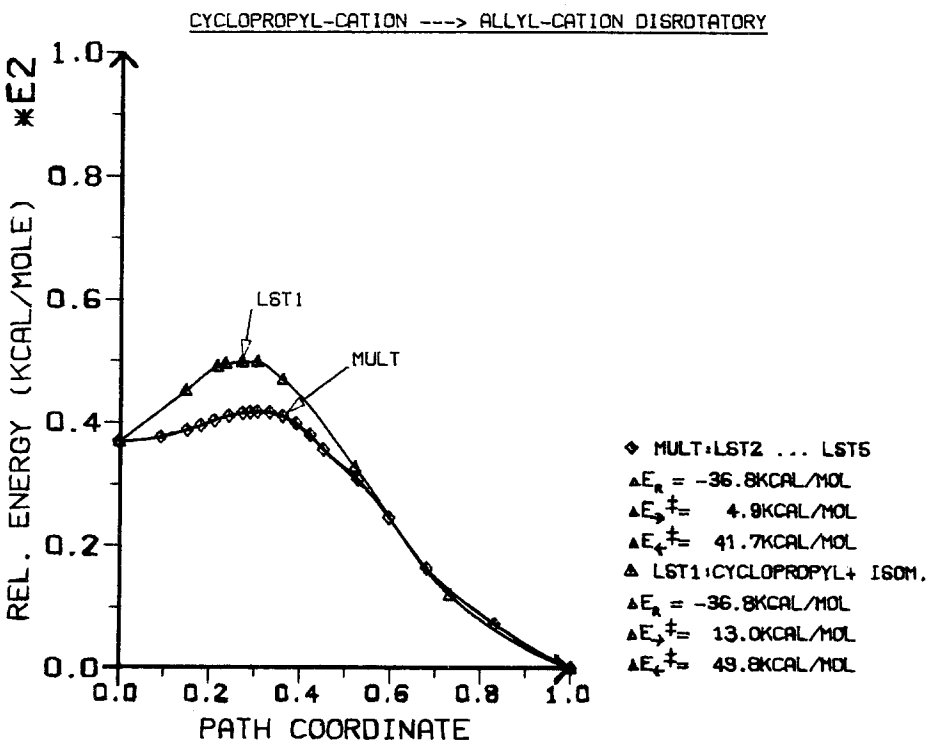


**Fig. 9.** Synchronous transit paths for the disrotatory interconversion of the cyclopropyl/allyl cation. MULT is the final multi-segment path (LST2 · · · LST5) which was constructed in the same way as described for the cyclobutene isomerization (Fig. 12) in the text

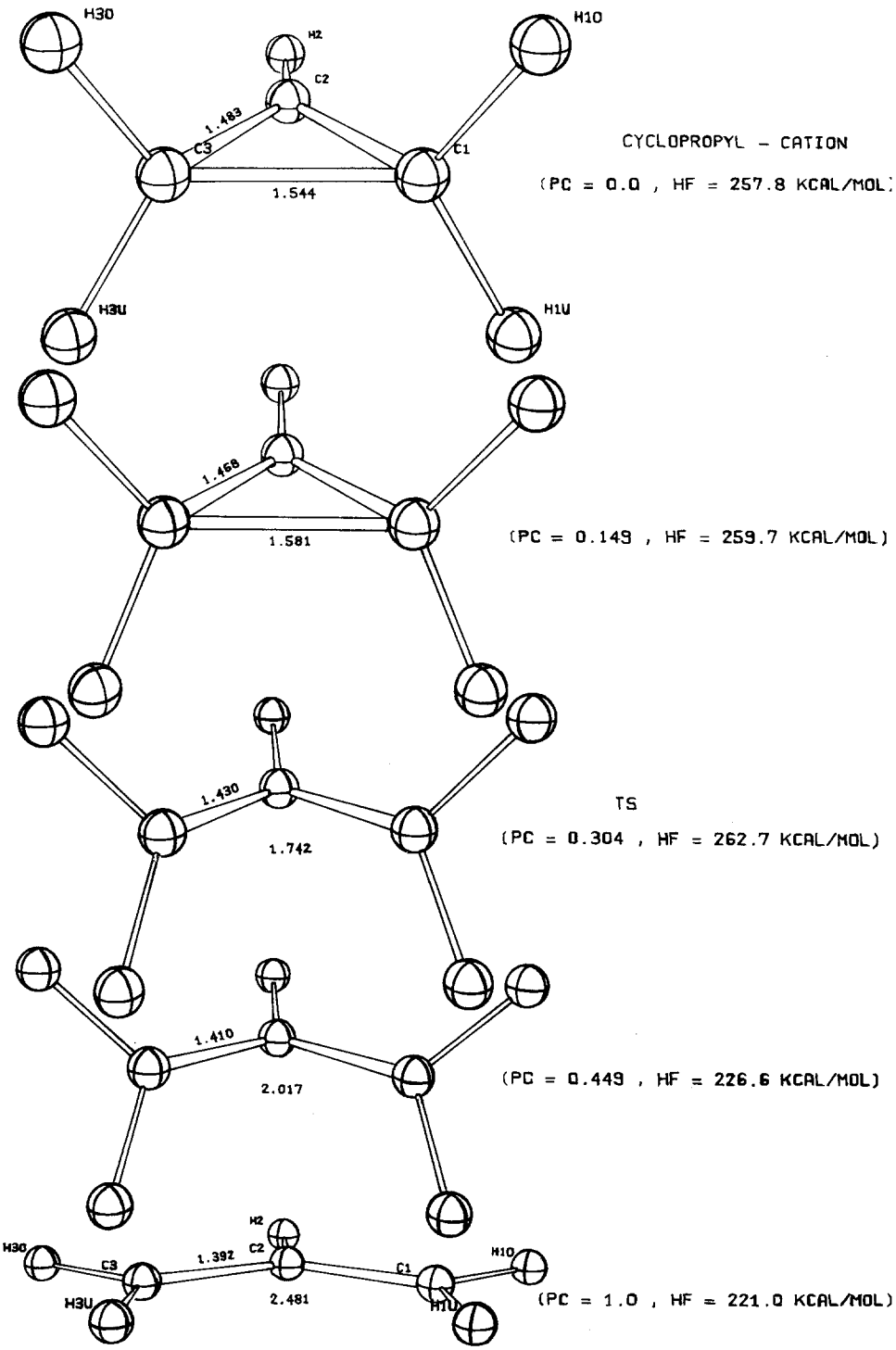


**Fig. 10.** ORTEP plots of the optimized path limiting structures for the synchronous transit segments (LST2 · · · LST5) of the disrotatory interconversion of the cyclopropyl/allyl cation

The first LST- and the final multi-segment path are shown in Fig. 9. The composite path was generated by orthogonal optimization of two points on each side of the transition state with PC = 0.304. In agreement with the Hammond postulate, this corresponds to a transition state in the vicinity of the reactant. In Figure 10 ORTEP plots of all optimized structures are displayed to illuminate the molecular changes in the course of reaction along the final multi-segment path given in Fig. 9.

### 6.2. *Cyclobutene → Butadiene (gauche)* [18]

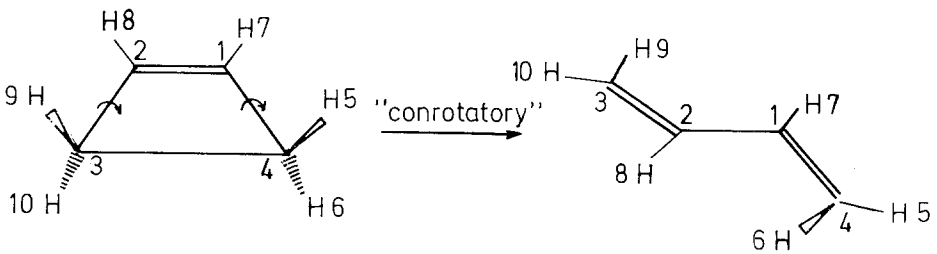


As previously mentioned, maximum coincidence according to PLM is demonstrated in Fig. 11 for cyclobutene and butadiene (gauche).

Results for the activation energy of ring opening and the geometry of the transition state are given in Tables 4 and 5. The path coordinate of the transition

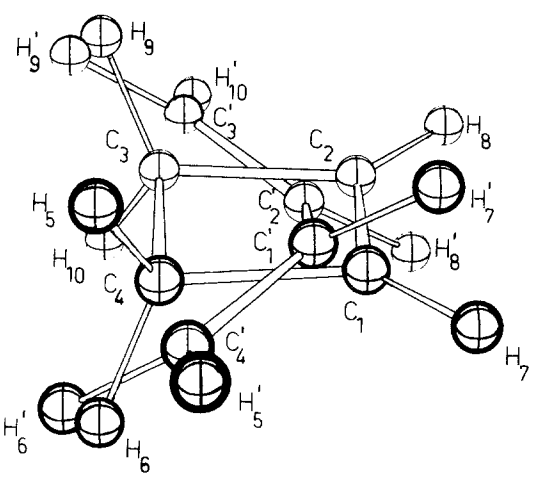


**Fig. 11.** PLM orientation of butadiene (gauche) relative to cyclobutene

**Table 4**

| Activation energy (kcal/mole) | SCF method | Search strategy |
|---|---|---|
| 49.9 | MNDO [18] | MINIMAX [16] |
| 49.9 | MNDO [6] | Gradient norm minimization |
| 85–88 | PRDDO [3b] | Orth. opt. + segmentation |

**Table 5**

| Parameter | MINIMAX | Ref. [6] |
|---|---|---|
| C1C4 | 1.417 | 1.417 |
| C1C2 | 1.408 | 1.406 |
| C3C4 | 2.123 | 2.117 |
| C2C1C4 | 103.3 | 103.1 |
| C3C4C1 | 74.5 | 74.5 |
| C4C1C2C3 | 21.2 | 22.6 |

*CiCjCkCl* = dihedral angle between atoms C*i*, C*j*, C*k*, C*l* in degrees.

state is 0.376 which is shifted (relative to reaction 6.1) to the product side, again in accord with the Hammond postulate.

One important difference is seen from Table 3: While MINIMAX achieves saddle point location without path segmentation, this is not true for orthogonal optimization. Nevertheless, path segmentation is necessary if the true minimum energy path is to be determined within sufficiently narrow limits.

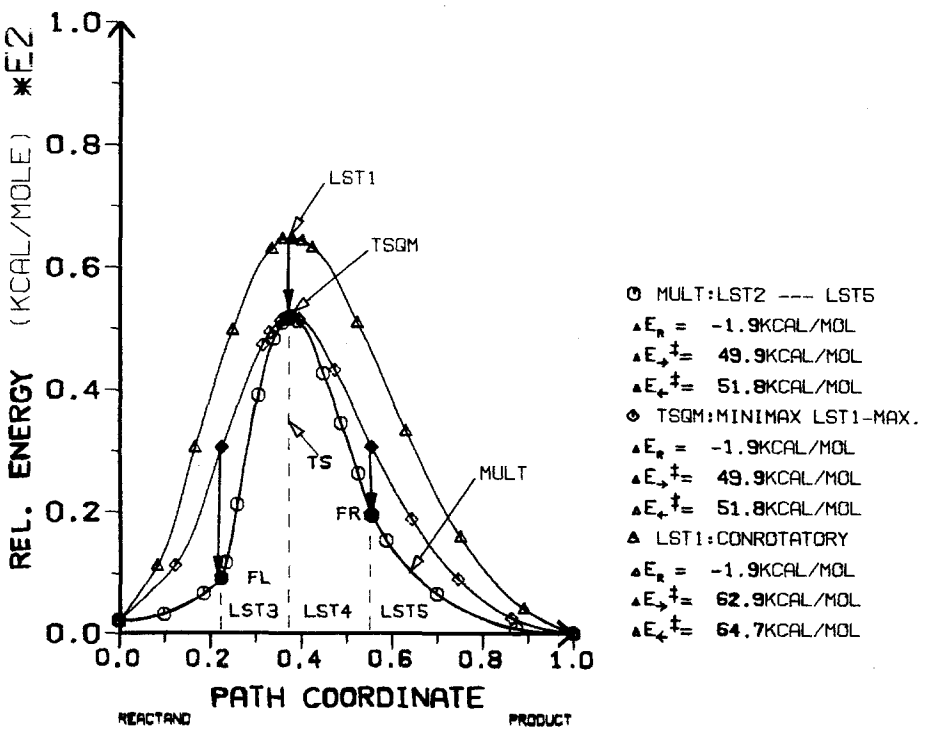


**Fig. 12.** Calculation of the final multi-segment path (LST2 · · · LST5) for the conrotatory interconversion of cyclobutene/butadiene (gauche). MINIMAX optimization of the LST1 maximum structure results (vertical arrow) in the QST path (TSQM) through the transition state TS. Orthogonal optimization of two geometries on each side of the transition state gives the new structures FL and FR (vertical arrows) which are used to construct the final segmented path

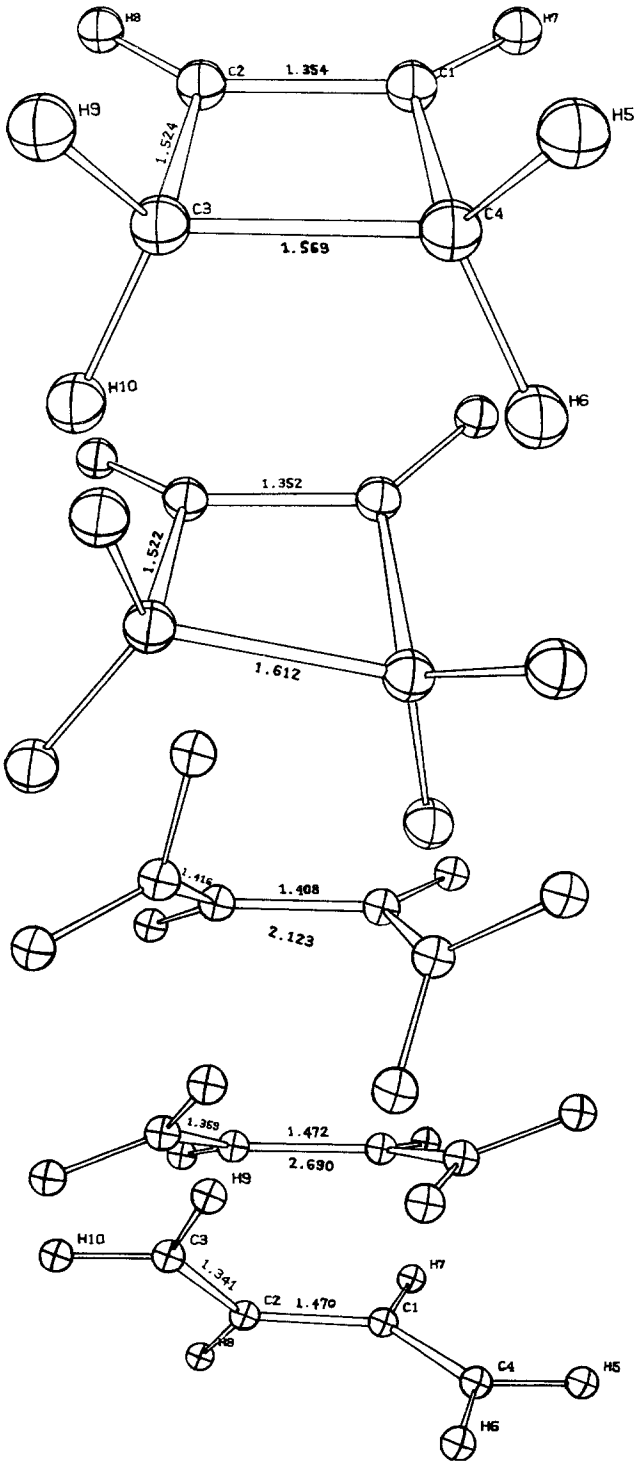


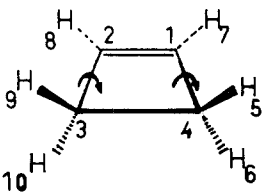


(PC = 0.0 , HF = 30.5 KCAL/MOL)

(PC = 0.225 , HF = 37.6 KCAL/MOL)

TS

(PC = 0.376 , HF = 80.3 KCAL/MOL)

(PC = 0.555 , HF = 47.9 KCAL/MOL)

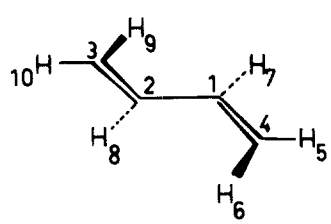


(PC = 1.0 , HF = 28.6 KCAL/MOL)

**Fig. 13.** ORTEP plots of the optimized path limiting structures for the synchronous transit segments (LST2 · · · LST5) of the conrotatory interconversion of cyclobutene/butadiene (gauche)

This procedure is summarized in Fig. 12, and the corresponding optimized structures are given as ORTEP plots in Fig. 13. For a closer comparison with the work of Halgren and Lipscomb (only graphic data published) a corresponding diagram for the variation of key parameters along the final multi-segment path (LST2 · · · LST5) is given in Fig. 14. The reader who is interested in more details is referred to Ref. [3b]. As a result, and despite the different SCF methods in use, a close analogy in the final reaction mechanism is found.

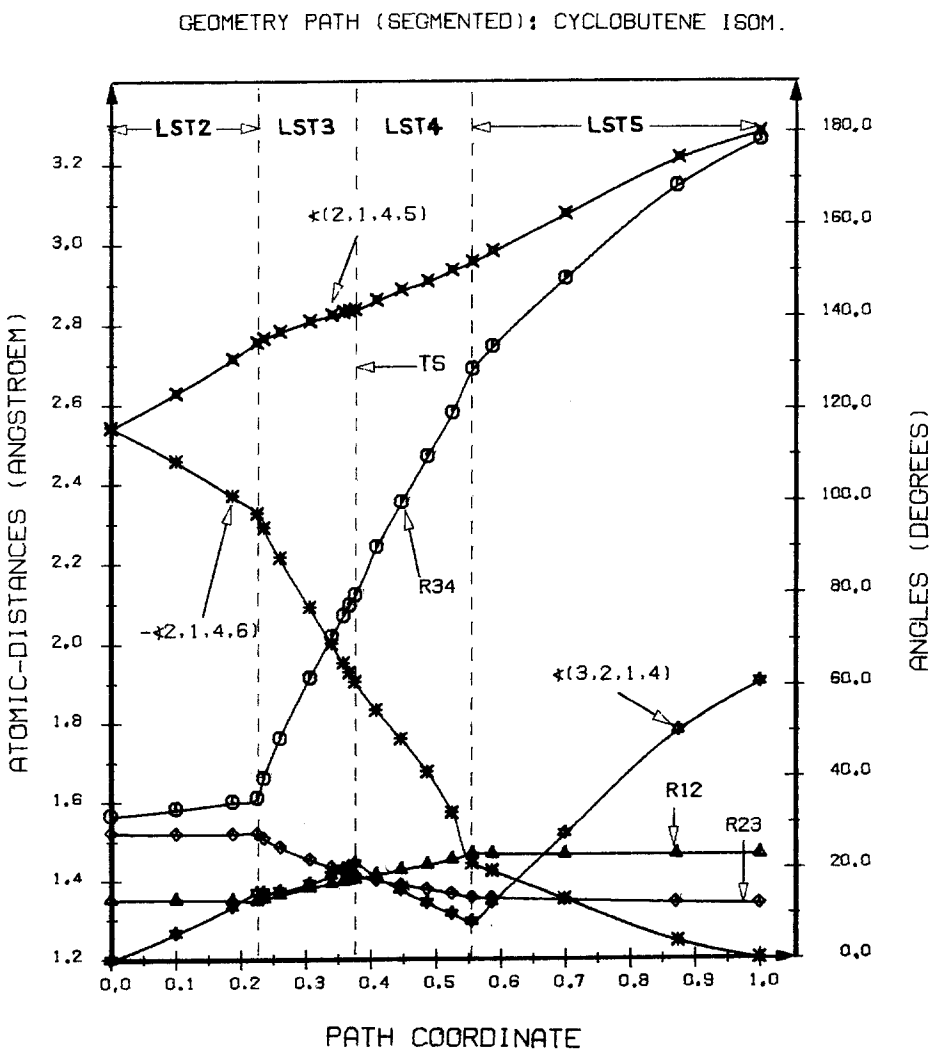


**Fig. 14.** Variation of key-geometric parameters for the conrotatory interconversion of cyclobutene/butandiene (gauche) along the final multi-segment path

## 7. Conclusion

Although far from being perfect, the concept of synchronous transit in conjunction with the principles of path segmentation, orthogonal, and MINIMAX/MINIMI optimization, proves to be a powerful tool for calculation of complicated energy hypersurfaces without the need of further information. As demonstrated for two-dimensional model surfaces and two electrocyclic reactions, the crucial problems such as the location of transition states and/or intermediates as well as a close approach to the steepest-descent path may be solved successfully within one method and hence within one program unit.

Over and above the merits already published [3b], its flexibility should be especially mentioned as an essential feature of the method:

- Energy gradients are dispensed with; total independence of quantum chemical description (SCF program in use).
- The method can be used automatically; on the other hand stepwise approximation to the "best solution" may be preferred for individual problems and SCF programs.
- Highly asynchronous or forbidden processes may be described.
- Parts of the molecule can be excluded from optimization [16] in order to diminish computational effort or to study the mechanistic consequences of this constraint.

Parallel to the present work, more than thirty transition states and reaction paths, mainly on the field of pericyclic reactions, have been explored without difficulty. Results of this work are in preparation [21].

All calculations were done with a Honeywell Bull 66/80 computer on the Universitäts Rechenzentrum Mainz. A scholarship of the Degussa AG/Frankfurt is gratefully acknowledged. The author especially thanks Professor H. Kunz (Universität Mainz) and Dr. A. Lawson (Beilstein Institut für Literatur der Organischen Chemie, Frankfurt/M.) for helpful discussions and comments on the manuscript.

## References

1. Quantum Chemistry Program Exchange, QCPE, Department of Chemistry, Indiana University, Bloomington, Ind.
2. a. Halgren, T. A., Kleier, D. A., Hall Jr., J. H., Brown, L. D., Lipscomb, W. N.: J. Am. Soc. **100**(21), 6595 (1978); b. Dewar, M. J. S., Ford, G. P.: J. Am. Chem. Soc. **101**(19), 5558 (1979)
3. a. Halgren, T. A., Pepperberg, I. M., Lipscomb, W. N.: J. Chem. Soc. **97**(5), 1248 (1975); b. Halgren, T. A., Lipscomb, W. N.: Chem. Phys. Letters **49**(2), 225 (1977)
4. Mueller, K., Brown, L. D.: Theor. Chim. Acta (Berl.) **53**, 75 (1979)
5. Mueller, K.: Angew. Chem. **92**, 1 (1980)
6. Thiel, W.: J. Am. Chem. Soc. **103**, 1420 (1981)
7. a. Ehrenson, S.: J. Am. Chem. Soc. **96**, 3778 (1974); b. Tee, O. S.: J. Am. Chem. Soc. **91**, 7144 (1969).
8. The formula (7) given in [3b] obviously is of wrong sign
9. PC = DR/(DR + DP) = const. = $p$ transforms with Eq. (1) to

$$(x + p^2 \cdot R/(1-2p))^2 + y^2 = ((1-p) \cdot p \cdot R/(1-2 \cdot p))^2$$

where $x_R = y_R = y_P = 0$, $x_P = R$

Middle points of the circles: $(-p^2 \cdot R/(1-2p), 0)$
Radii of the circles: $(1-p) \cdot p \cdot R/(1-2p)$

10. See 2a, 3b [Loc. cit. Ref. [4]] and [5] [lit. loc. cit.]
11. In the case of an orthogonal optimization, path segmentation means, according to Eq. (2) and [9], that the curvature of search radii relative to the energy hypersurface is changed
12. Ishida, K., Morokuma, K., Kormornicki, A.: J. Chem. Phys. **66**(5), 2153 (1977)
13. In principle, this could also be managed by an unconstrained optimization if one accepts the risk of convergence to product or reactant
14. Optimization of coordinates with step length 0.1 (for model surfaces), QST path maximum/minimum search with variable stepsize >0.015. Both quantities are unoptimized. Convergence was assumed if changes in the energy were less than 0.01 per cycle for model surfaces and 0.1 kcal/mole for molecules
15. Optimized with the constraint of $C_s$ symmetry (mirror plane through breaking bond)
16. As in [3b], C–H bond lengths were excluded from optimization. These quantities do not remain constant but vary linearly/parabolically along the transit paths
17. The MNDO program calculates energy gradients numerically by finite differences and was therefore modified to double precision arithmetic. This reduced the number of SCF calculations for some test molecules to one third
    a. Dewar, M. J. S., McKee, M. L., Rzepa, H. S.: J. Am. Chem. Soc. **100**, 3607 (1978)
    b. Dewar, M. J. S., Thiel, W.: Theor. Chim. Acta (Berl.) **46**, 89 (1977)
    c. Dewar, M. J. S., Thiel, W.: J. Am. Chem. Soc. **99**, 4907 (1977)
    d. Dewar, M. J. S., McKee, M. L.: J. Am. Chem. Soc. **100**, 7499 (1978)
18 It was not the aim to determine the absolute minimum conformation of butadiene (presumably transoid). A gauche conformation was chosen as starting point to detect a shallow minimum within the standard criteria of the MNDO program. In this way we wanted to test the suspicion of McIver and Kormornicki [19] that two different transition states for the ring opening exist, corresponding to the cisoid and transoid butadiene conformations. As far as comparison is possible, the transition state of these authors is virtually identical with ours and hence corresponds to the formation of cisoid butadiene
19. McIver, Jr., J. W., Kormornicki, A.: J. Am. Chem. Soc. **94**, 2625 (1972)
20. Optimized within the constraint of $C_2$-symmetry
21. Jensen, A., Kunz, H.: to be published

Received November 24, 1982